

MASTER OF SCIENCE THESIS

Finite Element Analysis of Cahn-Hilliard equations

Mass transfer of an oil-soluble chemical for water control

M. Gholami Gharasoo

July 27, 2005

Finite Element Analysis of Cahn-Hilliard equations

Mass transfer of an oil-soluble chemical for water control

MASTER OF SCIENCE THESIS

For obtaining the degree of Master of Science in Petroleum Engineering
and Geosciences at Delft University of Technology

M. Gholami Gharasoo

July 27, 2005



Delft University of Technology

Copyright © Department of Civil Engineering, Delft University of Technology
All rights reserved.

DELFT UNIVERSITY OF TECHNOLOGY
DEPARTMENT OF
APPLIED EARTH SCIENCE

The undersigned hereby certify that they have read and recommend to the Faculty of Civil Engineering and Geosciences for acceptance a thesis entitled “**Finite Element Analysis of Cahn-Hilliard equations**” by **M. Gholami Gharasoo** in partial fulfillment of the requirements for the degree of **Master of Science**.

Dated: July 27, 2005

Supervisors:

Dr. Fred Vermolen

Dr. Pacelli L.J. Zitha

Ir. Hein J. Castelijns

Readers:

Dr. J.D. Jansen

Dr. Pedro Rivera

Abstract

Two models have been constructed and physically motivated based on the (system of) Cahn-Hilliard equation(s) and Stefan problem in order to describe the behavior of fluids in a hypothetical mixture. A finite element method is developed to solve the Cahn-Hilliard equations based on a mixed formulation where reduction of the fourth-order spatial derivative is applied. The method is also extended to multiple species. Furthermore, mass conservation and energy decrease for the (system of) Cahn-Hilliard equation(s) as well as the Stefan problem are demonstrated mathematically. Then, all proved mathematical subjects have been verified by the numerical aspects for the purpose of approving the numerical results.

The Cahn-Hilliard equations with a diffuse interface has been compared to a Stefan problem with a sharp interface and a reasonable agreement is obtained. To find out the advantages and disadvantages, the results and assumptions are discussed at the end for both models.

Acknowledgments

I feel a deep sense of gratitude to all those who gave me the possibility to complete this thesis. I am deeply grateful for my direct supervisor Dr. Fred Vermolen from Mathematics Department of the TUDelft whose help, exhilarating suggestions and encouragement helped me in all the time of research. Besides, I am profoundly indebted to my other supervisors Dr. P. L. J. Zitha and Ir. Hein J. Castelijns from Applied Earth Science Department of the TUDelft, who helped me over this job for all their useful complimentary remarks and notifications. I also wish to express my great thanks to my classmates and friends in TUDelft specially to Habib Valiollahi and Ir. F. C. Schoemaker for their valuable comments.

Delft, University of Technology
July 27, 2005

M. Gholami Gharasoo

Table of Contents

Abstract	v
Acknowledgments	vii
Introduction	1
1 Physical Models	5
1-1 Mixture Properties	5
1-1-1 Definition of System	5
1-1-2 Free Energy	7
1-1-3 Diffusion	8
1-2 Stefan Problem	10
1-3 Comparison between the Models	12
1-3-1 Front Capturing	12
1-3-2 Front Tracking	12
2 Mathematical Properties	15
2-1 Properties of the CH system of equations	15
2-1-1 Mass Conservation	15
2-1-2 Energy Decrement	16
2-1-3 Concept of Phase Separation	16
2-2 Extension to Multi-component CH	17
2-2-1 Energy Decay for the Multi-component Case	18
2-3 Properties of the Stefan problem	19
2-3-1 Mass Conservation and Energy Decay	19
2-3-2 Free Energy Requirement	20

3	Numerical Methods	21
3-1	Numerical Solution Technique of the CH Equation	21
3-1-1	Problem formulation	21
3-1-2	Numerical Solution Method	22
3-2	Stefan Numerical Solution Technique	24
4	Results	27
4-1	The CH Binary Mixture	27
4-2	Multi-component Case	31
4-3	Stefan Problem for the Binary Solution	32
4-4	Comparison between a Stefan Problem and the CH Model	34
5	Conclusions	37
	Bibliography	39

List of Figures

1-1	Domain for a binary solution	6
1-2	Non-convex Free Energy Diagram	10
3-1	Galerkin linear test function, ψ vs. position x	23
4-1	Smoothing the initial condition	28
4-2	Results of the CH equation for a binary solution	29
4-3	Numerical verification for the CH properties	29
4-4	Interface motion in the CH equation	30
4-5	Comparison between the non-linear and the linear CH solutions	30
4-6	Eyre formula for a ternary mixture	31
4-7	Results of the Stefan problem for a binary solution	33
4-8	Numerical verification for properties of the Stefan problem	33
4-9	Comparison between the results of both models	35
4-10	Comparison between the interface change in each model	36

Introduction

Once we go ahead to consider the fluids interaction inside a multi-portion environment, we need to specify whether the components are miscible or immiscible. Here, The whole frame is considered as a hypothetical case of immiscible fluids. The immiscible mixture is separated into two phases by means of a sharp interface. The components of the mixture are soluble only in one of the phases depending on whether they are organic or inorganic. The immiscibility of fluids does not stop the diffusion through the interface but reduce it to infinitesimal extents. The process is aimed here to be figured out as a model by the help of the Cahn-Hilliard system of equations and a Stefan problem.

One of the structural problems in simulating the immiscible fluids behavior inside a mixture is to specify the position of interface together with its motion. The sort of transition that takes place in the mixture through the interface is determined by movement of the sharp interface. If the free energy of the homogeneous state is larger than the free energy of separated state, then the created miscibility gap causes in imperceptible changes of the composition of the mixture. As a result, the free energy of the mixture is gradually reduced and phase separation happens.

The specified model contains a narrow transition layer as a sharp interface in which the fluid may mix across it. The model describes the transport of the mixture components through the interface in which only diffusion influences its structure . A set of scalar fields are introduced as a identification for the mass concentration of the fluid components. Here, in this study we disregard the effect of convection on our model. But to have a complete model for every particular component, generally the change of mass concentrations resulting from total dissipation in the mixture is combined to the fluid motion equations to give a system of equations. The most well-known conjugated systems are the Euler (or Navier-Stokes) and Cahn-Hilliard equations. Dispersion is assumed to be a function of dimensional surface energy introduced as a non-locality term. Localized dissipation caused by mixing, represents the loss of solutions balance to the interface and provides the topological mechanism. Also the classical fluid equations can be applied on both sides of the interface and then jump conditions play a role across the interface.

In general, there is two types of sharp interface modeling, front tracking or front capturing. In this study, we use both methods to approach the problem. Finally, we do a comparison between the accuracy and stability of both methods. Normally in the front tracking method, the position of the interface is traced. Change of topology should be considered in both sides of transition layer. In some cases in which we have movement of the interface resulting in shrinkage or expansion of the geometrical form of domains. Clearly it is needed to retain their identity after this certain transformation.

In the front capturing method, a supplemental fourth order scalar field is added which helps to trace the transition layer between two fluid components by suppressing the effect of unstable region. In this method, topological changes of domains are free to be considered and the position of the interface is determined by smoothing the flow discontinuities. The easiness of use, computational success and lots of numerical ways to solve made it the favorable choice, notwithstanding all obstacles in solution dependencies on the type of smoothing of the flow discontinuities as well as sort of singularities which have to be taken.

The interface can be defined between two immiscible fluids as a very thin layer where unstable mixtures become stable by energy gradient terms. This idea was proposed first by Van der Waals [1894] and modified later by Cahn and Hilliard [1958] to be used in complex diffusional problems. In the Cahn-Hilliard basic form (purely diffusional), it is assumed that there is no coupling between fluid dynamics like diffusion and convection. The model is reliable enough to describe fluids well, however the effect of coupling is rather considerable due to the energy dependence on concentrations and related forces. The model proposed by Lowengrub and Truskinovsky [1998][15] takes this coupling into account, introducing two additional parameters. One parameter brings the effect of surface tension into account. The other parameter provides the mechanism for topological changes to handle the loss of regularity of the solutions. Another solution proposed by Chakrabarti et al.[11][12] and Brown and Chakrabarti[2] based on the Cahn-Hilliard-Cook model represents an extension of the Cahn-Hilliard equation by an additional noise term.

When we come to solve the set of partial differential equations, we have to consider how to deal with boundary conditions. Here, non-periodic conditions provide more descriptive results in phase separation phenomena (Chan and Rey, 1995)[17]. The zero mass flux on the border lines, considering no mass flow through them, creates suitable boundary condition. Furthermore, we need another set of boundary conditions to be able to solve the Cahn-Hilliard equation numerically. The natural boundary conditions can be applied as a particular option resulting from a symmetry argument.

In order to simulate smooth changes of topology, some abstract models have been introduced for diffusion equation. The most famous models are those of Ginzburg-Landau and Flory-Huggins which describe the free energy of a solution as a function of concentration gradients. Just the same, some other models have described energy dependency on density gradients rather than concentration gradients. Chakrabarti[3] used a fourth order energy model which was proposed by Ginzburg-Landau, yet did not consider the effect of geometry of the molecules. Brown and Chakrabarti[2] and Chakrabarti et al.[11][12] used the Flory-Huggins energy model [10] and limited their study to equal sizes of the molecules and the same degree of polymerization for each component. An

appropriate expression for the bulk free energy that can be used for polymers adequately, is the one due to Flory-Huggins. Flory-Huggins equation describes thermodynamics of the solutions which is based on the lattice theory. In this study we consider a non-symmetric phase diagram based on the Flory-Huggins equation, whose the non-symmetric shape arises from differences between molecular properties of the solution components.

Eyre [7] formulated a mathematical model for the multi-component version of phase transitions based on system of Cahn-Hilliard equations. The multiple phases may co-exist or compete together.

In this thesis, we explore some mathematical properties and numerical solutions of the Cahn-Hilliard equation. Further, we extend the mathematical properties and numerical solutions to multi-component systems. Finally, the relation between the Cahn-Hilliard equation and an appropriate Stefan problem is illustrated. This was done by use of a perturbation expansion by Pego [16] and the numerical validation is investigated here. The contents of this thesis are as follows. In Chapter 1, the governing equations are illustrated. In Chapter 2, the mathematical properties are investigated. In Chapter 3, the discrete schemes and the applied numerical methods are drawn. In Chapter 4, results are presented and compared. In Chapter 5, conclusions are drawn.

Chapter 1

Physical Models

1-1 Mixture Properties

1-1-1 Definition of System

Consider an immiscible (partly miscible) mixture when fluid components are separated by an interface in two phases. We need to define the domains of each phase as well as the position of the interface which separates the fluids. When separated state of fluids in solution leads to the lower amount of enthalpy than the homogeneous state of mixture, we have immiscible mixture at that certain temperature. Thus we consider a very simplified model of compressible and homogeneous fluids at a constant temperature, Figure 1-1. The motion of fluids can be modeled by use of either Euler or Navier-Stokes equations.

Hereinafter, we consider a solution composed of $N + 1$ components. Heterogeneous mixtures of several incompressible fluids can be pondered where the mass concentration is defined as $c_i = M_i/M$, $i \in \{1, \dots, N + 1\}$. M_i and V_i are masses and volumes of the constituents of mixture whose volume is V . Obviously as long as $M = M_1 + M_2 + \dots + M_{N+1}$, $c_1 + c_2 + \dots + c_{N+1} = 1$. We assume \mathbf{v}_i as fluids velocity which could be different and $\hat{\rho}_i = M_i/V$ as apparent densities. The mass balance equation for every component gives,

$$\frac{\partial \hat{\rho}_i}{\partial t} + \nabla \cdot (\hat{\rho}_i \mathbf{v}_i) = 0 \quad (1-1)$$

All actual densities $\rho_i = M_i/V_i$ then can be obtained by $\rho_i = \frac{V}{V_i} \hat{\rho}_i$. So generally we consider an isothermal system of incompressible fluids which form an ideal mixture. Therefore, no excess volume of mixing (i.e. for a binary solution $V_1 = \int_V \mathcal{H}(x) dx$ where \mathcal{H} is Heaviside function) and density can be described as $1/\rho = \sum_{i=1}^{N+1} c_i/\rho_i$. Mass-averaged velocity (or barycentric velocity) is introduced by $\rho \mathbf{v} = \sum_{i=1}^{N+1} \hat{\rho}_i \mathbf{v}_i$ when $\rho = \hat{\rho}_1 + \hat{\rho}_2 + \dots + \hat{\rho}_{N+1} = M/V$ is the entire density of mixture which changes if the

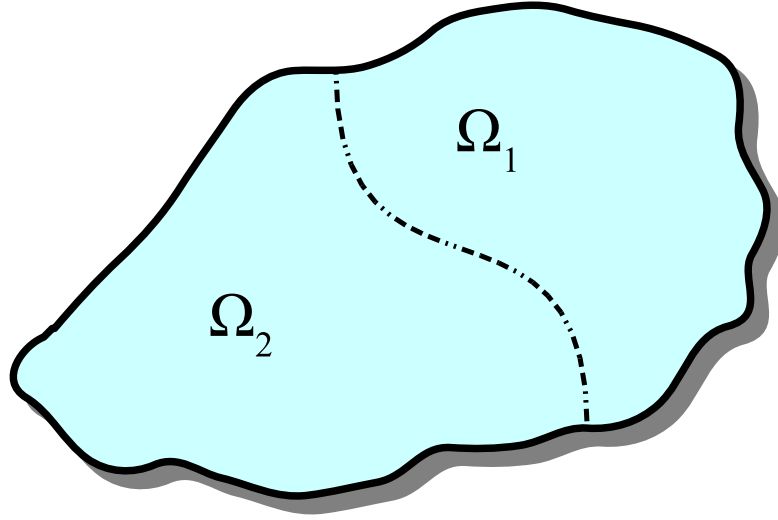


Figure 1-1: Simplified model of binary immiscible solution whose components separated by interface.

composition changes. As a consequence [15],

$$\frac{\partial \rho}{\partial t} + \nabla \cdot (\rho \mathbf{v}) = 0 \quad (1-2)$$

Now let us define a non-hydrostatic stress tensor \mathbf{P}_{nh} which has an additional stress term associated with the existence of concentration gradients (Cauchy stress), by

$$\mathbf{P}_{\text{nh}} := \left(-\rho^2 \frac{\partial f}{\partial \rho}\right) \mathbf{I} - \rho \nabla c \otimes \frac{\partial f}{\partial \nabla c} \quad (1-3)$$

where f is Helmholtz free energy,

$$f(\rho, \bar{c}, \nabla \bar{c}) = f_0(\rho, \bar{c}) + \frac{1}{2} \sum_{i=1}^N \kappa_{ii} |\nabla c_i|^2$$

which is obtained as Eq. (1-12) in the next section. Generalized chemical potential μ is defined by

$$\bar{\mu} = \frac{\partial f}{\partial \bar{c}} - \frac{1}{\rho} \nabla \cdot \left(\rho \frac{\partial f}{\partial \nabla \bar{c}} \right) \quad (1-4)$$

where the parameters including the overline, correspond to the vector of that quantity which consists of N elements. The linear conservation of momentum can be expressed by

$$\rho \frac{d\mathbf{v}_i}{dt} = \nabla \cdot \mathbf{P}_i \quad (1-5)$$

$$\forall i \in \{1, \dots, N+1\}$$

where \mathbf{P} is total stress tensor including non-hydrostatic stress \mathbf{P}_{nh} as well as viscous stress tensor $\mathbf{P}_{\mathbf{v}}$, given by

$$\mathbf{P}_{\mathbf{v}} = \eta (\nabla \mathbf{v} + \mathbf{v}^T) \quad (1-6)$$

Here η is shear viscosity. The notation $d/dt = \partial/\partial t + \mathbf{v} \cdot \nabla$ is used to denote the convective time derivative. Direct use of Eq. (1-3) results in another set of equations which describe the \mathbf{P}_{nh} dependency on Gibbs free energy $g(\rho, c, \nabla c)$ and concentration gradients [15],

$$\nabla \cdot \mathbf{P}_{\text{nh}} = -\rho(\nabla g - \mu \nabla c) \quad (1-7a)$$

$$g(\rho, c, \nabla c) = f + \rho \frac{\partial f}{\partial \rho} \quad (1-7b)$$

From Eq. (1-7a) and Eq. (1-5), the following equation is obtained for the acceleration,

$$\frac{d\mathbf{v}_i}{dt} = -\nabla g_i + \mu_i \nabla c_i + \frac{1}{\rho} \nabla \cdot (\mathbf{P}_{\mathbf{v}})_i \quad (1-8)$$

$\forall i \in \{1, \dots, N + 1\}$

1-1-2 Free Energy

The Helmholtz free energy \mathcal{F} of the mixture is the integral of the local free energy density f over the body Ω . Here f is assumed to be a function of \bar{c} and its gradient. A Taylor expansion up to the second order gives

$$f(\rho, \bar{c}, \nabla \bar{c}) = f_0(\rho, \bar{c}) + [\mathbf{L}] \cdot \nabla \bar{c} + [\mathbf{K}] |\nabla \bar{c}|^2 + \dots \quad (1-9)$$

Where $f_0(\rho, \bar{c})$ is the free energy density of a homogeneous system at concentration \bar{c} . Due to the symmetry center, $[\mathbf{L}]$ will be zero, since otherwise the value of f would be different for gradients in inverse direction. For isotropic system, the matrix $[\mathbf{K}]$ will be diagonal with equal elements, which can be taken as $\kappa/2$. In this simplified system the total free energy is

$$\mathcal{F}(\bar{c}) = \int_{\Omega} f(\rho, \bar{c}, \nabla \bar{c}) dA = \int_{\Omega} (\mathbf{K} |\nabla \bar{c}|^2 + f_0(\rho, \bar{c})) dA \quad (1-10)$$

Normally, the first term is referred to as the gradient penalty and the second one as homogeneous term [14]. For an infinite system, or one with periodic or Dirichlet conditions, we can obtain the potential μ from Eq. (1-4) for incompressible fluids as

$$\bar{\mu} = \frac{\delta \mathcal{F}}{\delta \bar{c}} = \frac{df_0}{d\bar{c}} - 2\mathbf{K} \nabla^2 \bar{c} \quad (1-11)$$

which results into Eq. (1-19) when combined with the diffusion flux equation Eq. (1-17). In case of immiscible fluids, high interaction parameters cause the free energy function $f(c)$ to be non-convex Figure 1-2. Therefore, in the concentration domain we have an unstable region where diffusivity is negative ($\mathcal{D}(c) = \nu d^2 f/dc^2 < 0$) and this implies spinodal decomposition to happen. Negative diffusion factors lead to problems

since they imply uphill diffusion. To tackle the problem, Cahn & Hilliard added the fourth order concentration gradient including κ to the free energy formulation as in Eq. (1-11). The term sometimes is called weak non-locality as well. κ is a very small positive number which can be obtained from measurement of the surface tension [5]. Some theories have been developed to predict κ as a function of concentration profile and physical properties of the molecules, like de Gennes(1980)[4], McMaste(1975) and Binder(1983)[1].

Practically, from Eq. (1-10) the local specific Helmholtz free energy for the mixture of $N + 1$ components can be obtained by

$$f(\rho, \bar{c}, \nabla \bar{c}) = f_0(\rho, \bar{c}) + \frac{1}{2} \sum_{i=1}^N \kappa_{ii} |\nabla c_i|^2 \quad (1-12)$$

where homogeneous contribution of free energy, f_0 is defined by Flory-Huggins in terms of volume fractions as [10]

$$f_0(\bar{\phi}) = RT \left(\sum_{i=1}^{N+1} \frac{\phi_i \ln \phi_i}{r_i} + \sum_{i=1}^N \sum_{j=i+1}^N \chi_{ij} \phi_i \phi_j \right) \quad (1-13)$$

R is the gas constant and χ_{ij} are physically dimensionless numbers which denote the interaction parameters. The Eq. (1-13) already considered the difference between the molecules of mixture components in term of their size by including term $r_i = V_i^m/V^m$ (V^m is the molar volume). To change from Flory-Huggins expression in terms of volume fractions Eq. (1-13) to Eq. (1-14) in terms of mass concentrations, we use $\phi_i = \rho c_i / \rho_i$. Hence,

$$f_0(\rho, \bar{c}) = RT \left(\sum_{i=1}^{N+1} \frac{c_i \ln c_i}{\mathcal{N}_i} + \sum_{i=1}^{N+1} \sum_{j=i+1}^{N+1} \chi_{ij} c_i c_j \right) \quad (1-14)$$

where $\mathcal{N}_i = (V_i^m/V^m)(\rho_i/\rho)$ is a dimensionless value chosen to reflect the relative molecular size and weight of component i . Regularly when the fluids are immiscible, the interaction parameters χ_{ij} are larger than the critical value χ_{ij}^{cr} , which is a function of the relative size of molecules. For a binary solution χ_{ij}^{cr} is defined by [5]

$$\chi_{ij}^{cr} = \frac{\mathcal{N}_i + \mathcal{N}_j + \sqrt{9\mathcal{N}_i^2 + 9\mathcal{N}_j^2 - 14\mathcal{N}_i\mathcal{N}_j}}{2\mathcal{N}_i\mathcal{N}_j} \quad (1-15)$$

In multi-component solutions when one of the χ_{ij} values becomes larger than χ_{ij}^{cr} , those i^{th} and j^{th} components act as immiscible fluids inside the mixture at that certain condition. To know more about critical phase behavior of the mixtures particularly binary solutions, see Gunton et al.[13].

1-1-3 Diffusion

The theory should include the possibility of mixing of the fluids, thus we need to introduce concentration as a scalar field which depends on position and time. The

general idea is to couple a diffusion model to the fluid motion model in order to construct fully physically motivative model of mixtures. Nevertheless to have a simplified model, we assume no velocity is induced due to concentration changes, $\mathbf{v} = 0$. Accordingly we take whole system as a density-matched system and we assume there is no external fluid field. All together we disregard the equation for the balance of momentum Eq. (1-8) which is resulting in $(d/dt) = (\partial/\partial t + \mathbf{v} \cdot \nabla) = (\partial/\partial t)$.

We need to make some assumption about the energy of mixing. A cardinal point about the fluid mixtures is that a certain degree of miscibility exists between the immiscible fluids even at low temperatures. A miscibility gap happens when the enthalpy of the homogeneous situation of mixture is greater than the enthalpy of separated state of phases in the mixture. If the temperature increases to critical temprature, the so-called equilibrium concentrations approach each other and miscibility gap that occurs at interface decreases. Above the critical temperature miscibility gas vanishes and system acts like a continuous mixture whose fluids are fully miscible. The change in topology is because of the system's desire to go to lowest level of energy. So the mixing models have been described by change of specific free energy which is presumed to be convex if fluids are miscible and non-convex if fluid are immiscible (section 1-1-2). At equilibrium, an immiscible mixture will separate into two phases having the binodal compositions. The method of determining binodal concentrations is founded on the common tangent construction of the Gibbs or Helmholtz free energy function, Eq. (1-9),

$$\left. \frac{df}{dc} \right|_{c_L} = \left. \frac{df}{dc} \right|_{c_R} \quad (1-16)$$

For a binary solution the position of binodal points and spinodal points are shown related to the energy digram in Figure 1-2. We need an additional equation of $c(x, t)$ for the purpose of describing the continuous change of concentration profiles in time. The diffusion equations can describe the dissipation due to the movement of the fluids and likewise fulfill the equilibrium conditions Eq. (1-16). Hence

$$\rho \frac{\partial \bar{c}}{\partial t} = \nabla \cdot (\bar{\mathbf{J}}), \quad \bar{\mathbf{J}} = \nu \nabla (\bar{\mu}) \quad (1-17)$$

where $\nu \geq 0$ is the mobility coefficient and $\bar{\mathbf{J}}$ is the tensor of diffusional flux. Equilibrium is achieved when chemical potentials are equal everywhere. Accordingly, substitution of Eq. (1-4) in balance equation Eq. (1-17), gives

$$\left\{ \begin{array}{l} \rho \frac{\partial c_i}{\partial t} = \nabla \cdot \left(\nu \nabla \left(\frac{\partial f}{\partial c_i} - \frac{1}{\rho} \nabla \cdot \left(\rho \frac{\partial f}{\partial \nabla c_i} \right) \right) \right) \\ \frac{\partial f}{\partial \nabla c_i} := \left\langle \frac{\partial f}{\partial \left(\frac{\partial c_i}{\partial x} \right)}, \frac{\partial f}{\partial \left(\frac{\partial c_i}{\partial y} \right)}, \frac{\partial f}{\partial \left(\frac{\partial c_i}{\partial z} \right)} \right\rangle \\ \forall i \in \{1, \dots, N\} \end{array} \right. \quad (1-18)$$

which is known as the Cahn-Hilliard equation. For making things easier, generally we assume the compressibility of the fluids to be negligible. Then for the incompressible

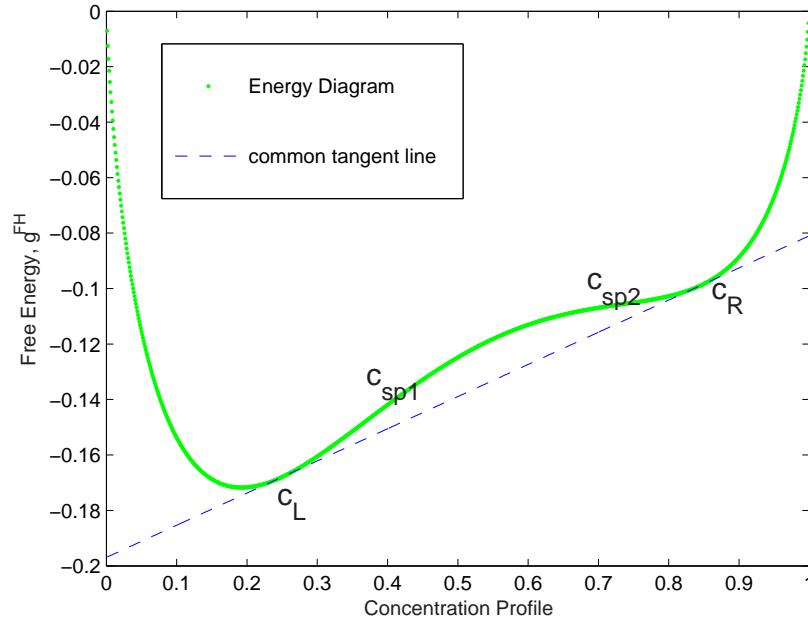


Figure 1-2: Binodal Points, $c_L = 0.2479$ and $c_R = 0.8443$ exist for critical binary solution when $\chi = 2.3 > \chi^{cr}$, $\mathcal{N}_1 = 0.8$, $\mathcal{N}_2 = 1.3$. c_{sp1} and c_{sp2} are spinodal (inflection) points where f'' is zero.

mixtures considering the free energy definition Eq. (1-11), Eq. (1-18) is rewritten as

$$\rho \frac{\partial c_i}{\partial t} = \nabla \cdot \left(\nu \nabla \left(\frac{\partial f_0}{\partial c_i} - \sum_{j=1}^N \kappa_{ij} \nabla^2 c_j \right) \right) \quad (1-19)$$

$\forall i \in \{1, \dots, N\}$

where f is the specific Helmholtz free energy Eq. (1-12) and the potential μ can be considered as the driving force for local changes of concentrations. Considering some assumptions, in the multi-component case, the model is proved numerically to be fully compatible with equilibrium condition Eq. (1-16). The CH equation and other later modified versions of that, are developed to describe the both non-critical and critical behavior of mixtures which latter leads to phase separation and spinodal decomposition.

1-2 Stefan Problem

Mass conservation of the components of mixture in whole domain of Ω , can be expressed as

$$\frac{d}{dt} \int_{\Omega} \bar{c} \, dV = 0 \quad (1-20)$$

In case the fluids are immiscible, we assume a sharp interface between phases which includes the unstable region. Therefore, concentration values at the sides of interface

where dissipation occurs, can never be a value between binodal points. Now, we drive the Stefan problem for a one-dimensional configuration. Derivation is similar for every component in the mixture so we write it generally in term of c where c could be every c_i , $\forall i \in \{1, \dots, N + 1\}$. Consider a sharp interface $S(t)$, over which the concentration is discontinuous with binodal points of c_L and c_R such that $\lim_{x \rightarrow S^-(t)} c(x, t) = c_L$ and $\lim_{x \rightarrow S^+(t)} c(x, t) = c_R$. Keeping Eq. (1-20) in mind and splitting it up into two parts $x < S(t)$ and $x > S(t)$, then it follows that

$$\frac{d}{dt} \int_{\Gamma_1}^{S(t)} c \, dx + \frac{d}{dt} \int_{S(t)}^{\Gamma_2} c \, dx = 0 \quad (1-21)$$

where Γ_1 and Γ_2 denote the left and right outwards boundaries of domain respectively. At the boundaries $x = \Gamma_1$ and $x = \Gamma_2$, we assume due to symmetry arguments that $\frac{\partial}{\partial x} = 0$. Application of Leibnitz' Rule gives

$$c_L S'(t) + \int_{\Gamma_1}^{S(t)} \frac{\partial c}{\partial t} \, dx + \int_{S(t)}^{\Gamma_2} \frac{\partial c}{\partial t} \, dx - c_R S'(t) = 0 \quad (1-22)$$

Substitution of the Cahn-Hilliard equation into the integrals in the Eq. (1-22), yields

$$\begin{aligned} S'(t)(c_L - c_R) + \int_{\Gamma_1}^{S(t)} \frac{1}{\rho} \frac{\partial}{\partial x} \left(\nu \frac{\partial}{\partial x} \left(f'_0(c) - \kappa \frac{\partial^2 c}{\partial x^2} \right) \right) \, dx \\ + \int_{S(t)}^{\Gamma_2} \frac{1}{\rho} \frac{\partial}{\partial x} \left(\nu \frac{\partial}{\partial x} \left(f'_0(c) - \kappa \frac{\partial^2 c}{\partial x^2} \right) \right) \, dx = 0 \end{aligned} \quad (1-23)$$

Using the boundary conditions gives

$$S'(t) = \frac{\nu \frac{\partial}{\partial x} \left(f'_0(c_R) - \kappa \frac{\partial^2 c}{\partial x^2}(S_+(t), t) \right) - \frac{\partial}{\partial x} \left(f'_0(c_L) - \kappa \frac{\partial^2 c}{\partial x^2}(S_-(t), t) \right)}{c_L - c_R} \quad (1-24)$$

if $c_L \neq c_R$. In this step ν and ρ have been treated as constants. The above equation can be re-arranged into

$$\begin{aligned} S'(t) = \frac{\nu f''_0(c_R) \frac{\partial c}{\partial x}(S_+(t), t) - f''_0(c_L) \frac{\partial c}{\partial x}(S_-(t), t)}{\rho} \\ + \frac{\nu \frac{\partial^3 c}{\partial x^3}(S_-(t), t) - \frac{\partial^3 c}{\partial x^3}(S_+(t), t)}{\rho} \end{aligned} \quad (1-25)$$

As $\kappa \rightarrow 0$ and has a constant value, the definitions $\mathcal{D}_R = \nu f''_0(c_R)$ and $\mathcal{D}_L = \nu f''_0(c_L)$, under the assumption that all spatial partial derivatives exist, lead to the following relation

$$S'(t) = \frac{1}{\rho} \frac{\mathcal{D}_R \frac{\partial c}{\partial x}(S_+(t), t) - \mathcal{D}_L \frac{\partial c}{\partial x}(S_-(t), t)}{c_L - c_R} \quad (1-26)$$

which is known as the Stefan condition and it describes the rate of motion of the interface. The interface can move only when the initial condition is not as same as the binodal equilibrium and we have asymmetric shape of the free energy expression or initial condition. The magnitude of $c_L - c_R$ denotes the miscibility gap. Some numerical methods for Stefan problems have been proposed and analyzed by, among many others, F.J. Vermolen and C. Vuik [9][8].

1-3 Comparison between the Models

Accordingly, now we can summarize all the expressions together and write the closed system of equations. In this paper, two different approaches were employed to be solved numerically. One is based on the method of Cahn & Hilliard which is using an additional scalar field to capture the interface position. Another method is using an additional expression, the Stefan condition, to track the position of interface explicitly. Then, a comparison between the numerical results of both methods reveals the advantages and disadvantages of each.

1-3-1 Front Capturing

Collecting the mass balance equations and the CH diffusion equation together, gives a system of equations for a quasi-incompressible, isothermal and nonuniform fluid mixture as

$$\frac{\partial \rho}{\partial t} = -\rho \nabla \cdot \mathbf{v} \quad (1-27a)$$

$$\rho \frac{\partial c_i}{\partial t} = \nabla \cdot \left(\nu \nabla \left(\frac{\partial f_0}{\partial c_i} - \sum_{j=1}^N \frac{\kappa_{ij}}{\rho} \nabla \cdot (\rho \nabla c_j) \right) \right) \quad (1-27b)$$

$$\forall i \in \{1, \dots, N\}$$

where the mixture assumed to have $N+1$ components. To solve this system numerically, the symmetry boundary conditions are chosen as

$$[\nabla c] \cdot \mathbf{n} = 0 \quad (1-28a)$$

$$[\nabla(\Delta c)] \cdot \mathbf{n} = 0 \quad (1-28b)$$

which represents natural boundary conditions and zero mass flux boundary conditions. \mathbf{n} is the unit normal vector perpendicular to the boundaries.

1-3-2 Front Tracking

The diffusion equation Eq. (1-17) can be written as

$$\rho \frac{\partial c}{\partial t} = \frac{\partial}{\partial x} \left(\mathcal{D}(c) \frac{\partial c}{\partial x} \right) \quad (1-29)$$

where $\mathcal{D}(c) = \nu d^2 f / dc^2$ is the diffusion coefficient. Since we consider the transition layer apart from domains where diffusion occurs locally and the interface is tracked separately, then the term for dispersion (weak non-locality κ) can be neglected. Therefore, the diffusion coefficient can be regarded as $\mathcal{D}(c) = \nu d^2 f_0 / dc^2$.

This Stefan problem Eq. (1-26) describes the movement of front due to the asymmetry of free energy diagram or initial condition when initial conditions essentially are different from the values of binodal concentrations. Clearly, this leads to expansion or shrinkage of the domains where regular dissipation occurs, and defines the position of nodes (or ranges) where concentration profiles numerically figured out, to be function of time. As a result, concentration profiles can be expressed as $c = c(x(t), t)$. Therefore

$$\frac{dc}{dt} = \frac{\partial c}{\partial t} + \frac{\partial c}{\partial x} x_t(t) \quad (1-30)$$

Having Eq. (1-30), then easily Eq. (1-29) takes the form

$$\frac{dc}{dt} - \frac{\partial c}{\partial x} x_t(t) = \frac{1}{\rho} \frac{\partial}{\partial x} \left(\mathcal{D}(c) \frac{\partial c}{\partial x} \right) \quad (1-31)$$

The Stefan problem (Eq. (1-26)) determines the velocity profile $x_t(t)$ which has its maximum at interface $dS(t)/dt$. Here $x_t(t)$ is defined as the velocity of the gridnodes. This will be clarified in Chapter [3]. Velocity decreases as it goes to the boundaries where there is no flux and natural boundary conditions are applied. We need another set of boundary conditions at interface. To satisfy the equilibrium condition Eq. (1-16) and to have positive values of diffusivity $f''(c) > 0$, we take binodal concentrations

$$c_R = c \Big|_{(x,y,z) \rightarrow S_+(t)}, \quad c_L = c \Big|_{(x,y,z) \rightarrow S_-(t)} \quad (1-32)$$

as the essential boundary condition for interface. Summarizing whole of model, we have

$$\frac{dc}{dt} = \frac{\partial c}{\partial x} x_t(t) + \frac{1}{\rho} \frac{\partial}{\partial x} \left(\mathcal{D}(c) \frac{\partial c}{\partial x} \right) \quad (1-33a)$$

$$\frac{dS(t)}{dt} = \frac{1}{\rho} \frac{\mathcal{D}_R \frac{\partial c}{\partial \mathbf{n}}(S_+(t), t) - \mathcal{D}_L \frac{\partial c}{\partial \mathbf{n}}(S_-(t), t)}{c(S_-(t)) - c(S_+(t))} \quad (1-33b)$$

where the following boundary conditions hold

$$\frac{\partial c}{\partial \mathbf{x}} = 0 \quad , \quad \text{for } \mathbf{x} \in \{\Gamma_1, \Gamma_2\} \quad (1-34a)$$

$$c \Big|_{S_+(t)} = c_R \quad (1-34b)$$

$$c \Big|_{S_-(t)} = c_L \quad (1-34c)$$

Mathematical Properties

2-1 Properties of the CH system of equations

2-1-1 Mass Conservation

The total mass of mixture should be conserved. This is crucial when we deal with a system of equations which describes the behavior of solutions. Here, theoretically we show that mass is conserved by the CH equation and later we see how numerically it does as well. Since there is no flux over the boundaries and that there are no internal sources, then we show that

$$\frac{d}{dt} \int_{\Omega} \bar{c} \, dA = 0 \quad (2-1)$$

As we go along, we prove that the CH equation pursue this circumstance. Substitution of Eq. (1-19) in Eq. (2-1) gives

$$\int_{\Omega} \frac{\partial \bar{c}}{\partial t} \, dA = \int_{\Omega} \nabla \cdot (\nu \{f_0''(\bar{c}) \nabla \bar{c} - 2\mathbf{K} \nabla(\Delta \bar{c})\}) \, dA \quad (2-2)$$

where \mathbf{K} is the non-locality tensor in the general form of free energy expression Eq. (1-9). Implementation of the Divergence Theorem on Eq. (2-2) yields

$$\int_{\Omega} \frac{\partial \bar{c}}{\partial t} \, dA = \int_{\partial \Omega} \nu \left\{ f_0''(\bar{c}) \frac{\partial \bar{c}}{\partial \mathbf{n}} - 2\mathbf{K} \frac{\partial(\Delta \bar{c})}{\partial \mathbf{n}} \right\} \, dS \quad (2-3)$$

The boundary conditions for CH equation Eq. (1-28a) & Eq. (1-28b) can be written in the following form

$$\frac{\partial \bar{c}}{\partial \mathbf{n}} = 0 \quad (2-4a)$$

$$\frac{\partial(\Delta \bar{c})}{\partial \mathbf{n}} = 0 \quad (2-4b)$$

Substitution of Eq. (2-4a) & Eq. (2-4b) into Eq. (2-3) reduces the CH equation to the prescribed form of mass conservation Eq. (2-1). Hence, in principle mass is conserved by the CH equation.

2-1-2 Energy Decrement

Fundamentally, to reach to the stable situation, the total energy of system should decrease. Thermodynamically, The entropy production and energy decline is the basic concept for every physical or chemical process to take place. Thus, it is imperative for physical models to be elaborated with respect to energy decrement. Here in a theoretical manner, we demonstrate energy reduction for the CH equation. Later on, we will see that numerical results satisfy theoretical conceptions. To make a beginning, the total energy is given by Eq. (1-10). Now we consider the decrease of total energy in the course of time for a binary mixture

$$\frac{d}{dt}\mathcal{F}(\bar{c}) = \int_{\Omega} \{f'_0(\bar{c}) - 2\mathbf{K}\Delta\bar{c}\} \frac{dc}{dt} dA \quad (2-5)$$

In the last step we used the Chain Rule for differentiation and we kept in mind that also a differentiation with respect to ∇c has to be carried out. The Cahn-Hilliard equation Eq. (1-19) can be represented by

$$\frac{\partial c}{\partial t} = M\Delta (f'_0(\bar{c}) - 2\mathbf{K}\Delta(\bar{c})) \quad (2-6)$$

Considering $\mathbf{v} = 0$ and $dc/dt = \partial c/\partial t$, then substitution of Eq. (2-6) into Eq. (2-5) yields

$$\frac{d}{dt}\mathcal{F}(\bar{c}) = M \int_{\Omega} (f'_0(\bar{c}) - 2\mathbf{K}\Delta\bar{c})\Delta(f'_0(\bar{c}) - 2\mathbf{K}\Delta\bar{c})dA = - \int_{\Omega} \|\nabla(f'_0(\bar{c}) - 2\mathbf{K}\Delta\bar{c})\|^2 dA \leq 0 \quad (2-7)$$

The last step follows from integration by parts and use of the boundary conditions. This implies that the total energy indeed decreases as time proceeds. This analysis is similar to the one by deMello et al [6].

2-1-3 Concept of Phase Separation

The exact locations of the binodal and spinodal points (or lines in case of a multi-component solution) in the free energy diagram can be derived from

$$\left. \frac{\partial^2 f_0}{\partial c^2} \right|_{SP} = 0 \quad (2-8a)$$

$$\left. \frac{\partial f_0}{\partial c} \right|_{BP1} = \left. \frac{\partial f_0}{\partial c} \right|_{BP2} \quad (2-8b)$$

As we see also in Figure 1-2 spinodal points (lines) Eq. (2-8a) are inflection points where the second derivative of free energy diagram is equal to zero. Binodal points are

external to the spinodal points and located close to minimum points (in a symmetric energy diagram they are exactly the minimum points). Eq. (2-8b) is similar to Eq. (1-16) for determining equilibrium points (lines).

When the temperature of mixture is brought below the critical temperature, the constituents are immiscible in the solution and phase separation possibly occurs. Two main processes which play an important role in phase separation occurrence, are nucleation & growth (NG) and spinodal decomposition (SD). In the metastable region which is defined as the area between binodal points (lines) and spinodal points (lines), the stability of solution is highly dependent on the amplitude and value of concentration fluctuations. Thus in metastable region, phase separation occurs through NG. However, the behavior in unstable region, which is located between the spinodal points is different. In this region, phase separation occurs through SD because contrary to the metastable region, even small perturbations of concentration can reduce the total free energy of the system. Therefore, we deal with a partly stable solution in the unstable region (see Gunton et al.) [13].

2-2 Extension to Multi-component CH

Extended CH equation for a multi-component solution which is presented here, mainly is based on the formula proposed by Eyre [7]. For a mixture with $N + 1$ components in a discretized domain of n parts, according to what we debate in Chapter (1) about diffusion and free energy, the generalized form of CH equation can be expressed as

$$\frac{\partial c_i(x, t)}{\partial t} = \Delta(\nabla_{c_i(x, t)} f_0(\bar{c}(x, t)) - \mathbf{\Gamma} \Delta \bar{c}(x, t)) \quad (2-9)$$

where

$$\bar{c} \in \mathcal{R}^N, \quad x \in \Omega \subset \mathcal{R}^n, \quad \mathbf{\Gamma} \in \mathcal{R}^{N \times N}, \quad f_0(\bar{c}) : \mathcal{R}^N \mapsto \mathcal{R} \quad (2-10)$$

The interaction matrix $\mathbf{\Gamma}$ is symmetric and holds the non-locality terms κ inside. According to Binder [1] the entries of matrix $\mathbf{\Gamma}$ generally depend on the mass concentrations and other physical factors, however the effect is assumed to be negligible, so we can treat them as constants. Natural boundary conditions and zero mass flux over the boundaries are considered for this system Eq. (1-28a) and Eq. (1-28b). So similarly we have

$$\frac{\partial c_i}{\partial \mathbf{n}} = 0 \quad (2-11a)$$

$$\frac{\partial}{\partial \mathbf{n}} (\Delta c_i) = 0 \quad (2-11b)$$

$$\text{where } i = \{1, \dots, N\}$$

In the Eq. (2-9), the mobility term ν/ρ is not involved or it is considered as a constant unit tensor, \mathbf{I} . Extension of Eq. (2-9) for $N + 1$ components yields

$$\frac{\partial c_i}{\partial t} = \nabla \cdot \left\{ \sum_{j=1}^N \left(\frac{\partial^2 f_0(\bar{c})}{\partial c_i \partial c_j} \nabla c_j - \nabla (\mathbf{\Gamma}_{ij} \Delta c_i) \right) \right\} \quad (2-12)$$

for all components in the mixture, $i \in \{1, \dots, N\}$. Direct calculation of the Flory-Huggins free energy formula Eq. (1-14) to get the diffusion factors, yields

$$\frac{\partial^2 f_0(\bar{c})}{\partial c_i \partial c_j} = \begin{cases} \frac{1}{\mathcal{N}_N \left(1 - \sum_{j=1}^N c_j\right)} + \frac{1}{\mathcal{N}_i c_i} - 2\chi_{i,N} & , \quad i = j \\ \frac{1}{\mathcal{N}_N \left(1 - \sum_{j=1}^N c_j\right)} + \chi_{i,j} - \chi_{i,N} - \chi_{N,j} & , \quad i \neq j \end{cases} \quad (2-13)$$

The same numerical method (Galerkin FEM) is employed in numerical chapter for the solution of multi-component case.

2-2-1 Energy Decay for the Multi-component Case

Now, we will show that the total energy decreases for the multi-component case as well. Following Eyre[7], consider the total energy

$$\mathcal{F}(\bar{c}) = \int_{\Omega} \{f_0(\bar{c}) + \frac{1}{2} \nabla \bar{c}^T \mathbf{\Gamma} \nabla \bar{c}\} dA = \int_{\Omega} g(\bar{c}, \nabla \bar{c}) dA \quad (2-14)$$

Then it can be shown that for each component we have

$$\frac{\delta g}{\delta c_i} = \frac{\delta f_0}{\delta c_i} - \sum_{j=1}^N \mathbf{\Gamma}_{ij} \Delta c_j \quad (2-15)$$

The Cahn-Hilliard equation can be written for each component by

$$\frac{\delta c_i}{\delta t} = M \Delta \frac{\delta g}{\delta c_i} = M \Delta \left[\frac{\delta f_0}{\delta c_i} - \sum_{j=1}^N \mathbf{\Gamma}_{ij} \Delta c_j \right] \quad (2-16)$$

$\forall i \in \{1, \dots, N\}$

Now, we compute the change of $\mathcal{F}(\bar{c})$ with respect to time

$$\frac{d}{dt} \mathcal{F}(\bar{c}) = \int_{\Omega} \sum_{i=1}^N \left\{ \frac{\delta g}{\delta c_i} \frac{\partial c_i}{\partial t} \right\} dA \quad (2-17)$$

using Eq. (2-16), we obtain

$$\frac{d}{dt} \mathcal{F}(\bar{c}) = M \int_{\Omega} \sum_{i=1}^N \left\{ \frac{\delta g}{\delta c_i} \Delta \frac{\delta g}{\delta c_i} \right\} dA = -M \int_{\Omega} \sum_{i=1}^N \left\{ \|\nabla \left(\frac{\delta g}{\delta c_i} \right)\|^2 \right\} dA \leq 0 \quad (2-18)$$

The last steps follow from application of the Product Rule for differentiation and the use of the boundary conditions. Herewith, it has been shown that the total energy decreases as a function of time.

2-3 Properties of the Stefan problem

2-3-1 Mass Conservation and Energy Decay

Mass is totally conserved in the Stefan problem because its proof is based on mass conservation. Here and now, we formulate a criterion for the Stefan problem to have a decrease of energy. Consider the Stefan problem where diffusion is described by

$$\frac{\partial c}{\partial t} = M\Delta f'(c) = M\nabla \cdot f''(c)\nabla c \quad (2-19)$$

under assumption that $\kappa \rightarrow 0$. Then the total energy is given by

$$\mathcal{F}(c) = \int_{\Omega} f(c) dA \quad (2-20)$$

for one-dimensional case the total change of energy has the form of

$$\frac{d}{dt} \int_{\Gamma_1}^{\Gamma_2} f(c) dx = \frac{d}{dt} \int_{\Gamma_1}^{S(t)} f(c) dx + \frac{d}{dt} \int_{S(t)}^{\Gamma_2} f(c) dx \quad (2-21)$$

Using Leibnitz' Rule for the differentiation with respect to time, one gets

$$\frac{d}{dt} \mathcal{F}(c) = (f(c(S^-(t), t)) - f(c(S^+(t), t))) S'(t) + \int_{\Gamma_1}^{\Gamma_2} f'(c) \frac{\partial c}{\partial t} dx \quad (2-22)$$

The last term is less or equal to zero as has been shown before. This implies that

$$(f(c_L) - f(c_R)) S'(t) \leq 0, \quad (2-23)$$

gives a sufficient condition that energy decreases. The sign of $S'(t)$ can be determined from a global mass balance Eq. (2-1). We have that

$$c_L^0(S^0 - \Gamma_1) + c_R^0(\Gamma_2 - S^0) = c_L(S^\infty - \Gamma_1) + c_R(\Gamma_2 - S^\infty) \quad (2-24)$$

Assuming monotonic behavior of $S(t)$, we see that the sign of $S'(t)$ equals the sign of $(S^\infty - S^0)$ where S^0 and S^∞ respectively denote the initial and final position of the interface. Hence, condition Eq. (2-23) amounts to

$$(f(c_L) - f(c_R)) (S^\infty - S^0) \leq 0 \quad (2-25)$$

From Eq. (2-24) it follows

$$S^\infty - S^0 = \frac{(\Gamma_2 - S^0)(c_R^0 - c_R) + (S^0 - \Gamma_1)(c_L^0 - c_L)}{c_L - c_R} \quad (2-26)$$

Herewith, Eq. (2-25) amounts to

$$(f(c_L) - f(c_R)) \frac{(\Gamma_2 - S^0)(c_R^0 - c_R) + (S^0 - \Gamma_1)(c_L^0 - c_L)}{c_L - c_R} \leq 0 \quad (2-27)$$

which poses a sufficient condition for the Stefan problem to yield a decreasing total energy under assuming $\kappa \rightarrow 0$. The consequences of binodal and spinodal points to negative diffusivity are useless here, because the computational domains considered to be located always in the stable region. Later we will discuss the numerical method to get to the solution of the Stefan problem.

2-3-2 Free Energy Requirement

The diffusivity equation Eq. (1-17) is the basic equation for both CH Equation (Eq. (1-27b)) as the Stefan problem (Eq. (1-33a)). Here we discuss the essential conditions mainly for the free energy diagram to have a steady state solution for both miscible and immiscible mixtures. Consider Eq. (1-17) in a one-dimensional domain limited by boundaries Γ_1 and Γ_2 . Also we take $\kappa = 0$ in this analysis. At the certain time step $t \rightarrow \infty$, we suppose that a steady state solution exists over the domain and the boundaries have the concentration values $c(\Gamma_1, t) = c_{\Gamma_1}$ and $c(\Gamma_2, t) = c_{\Gamma_2}$. We denote the steady-state solution by \check{c} i.e. $\lim_{t \rightarrow \infty} c(x, t) = \check{c}$, then the Eq. (1-17) takes the following form

$$0 = \frac{\partial}{\partial x} \left(f_0''(\check{c}) \frac{\partial \check{c}}{\partial x} \right) \quad (2-28)$$

Integration of Eq. (2-28) over position easily gives,

$$\int_{c_{\Gamma_1}}^{\check{c}} f_0''(c) dc = A(x - \Gamma_1) \quad (2-29)$$

where A is a constant value. Substitution of the boundary values into Eq. (2-29) yields two different equations

$$f_0'(\check{c}) - f_0'(c_{\Gamma_1}) = A(x - \Gamma_1) \quad (2-30a)$$

$$f_0'(c_{\Gamma_2}) - f_0'(c_{\Gamma_1}) = A(\Gamma_2 - \Gamma_1) \quad (2-30b)$$

Combination of Eq. (2-30a) and Eq. (2-30b) gives the definition of the position as a function of the concentration and the free energy

$$\frac{x - \Gamma_1}{\Gamma_2 - \Gamma_1} = \frac{f_0'(\check{c}) - f_0'(c_{\Gamma_1})}{f_0'(c_{\Gamma_2}) - f_0'(c_{\Gamma_1})} \quad (2-31)$$

According to Eq. (2-31), \check{c} is obtained by the inverse function of f_0' and the following principles are stated:

- $f_0'(\check{c})$ should be invertible on domain $[\Gamma_1, \Gamma_2]$, otherwise there is no smooth solution.
- For the case there is a $\check{c}_* \in [c_{\Gamma_1}, c_{\Gamma_2}]$ for which $f_0''(\check{c}_*) = 0$, then according to the Implicit Function Theorem there is no smooth solution.

where the second one is the case happens for immiscible fluids markedly because of the unstable zone presence, see Figure 1-2. This short mathematical note clearly proves the importance of the forth order term with κ to suppress the unphysical effect of the unstable region on the solution.

Chapter 3

Numerical Methods

To solve the models numerically, the Galerkin's finite element method is used. The FEM has some advantages over finite difference method (FDM). First it is easier to expand the solution for more dimensions, specially for odd geometries. Further, the FEM allows us to deal with discontinuities of coefficients in a natural way. In this study we used Galerkin's FEM for both models.

3-1 Numerical Solution Technique of the CH Equation

3-1-1 Problem formulation

In this paper, we disregard the effect of acceleration terms on dissipation. So the formulation is limited to the solution of CH equation considering proper initial and boundary conditions. The solution is limited to the one-dimensional study, bounded to a column with dimension of L . Furthermore, the mobility ν , interaction parameters χ_{ij} and the weak non-locality term κ are assumed to be constant. The size of molecules for each fluid in the mixture is different resulting a non symmetric energy diagram. The scalar fields $c_i(x, t)$ are dependent variables where $i = 1, \dots, N$ for a mixture with $N + 1$ components. All quantities are related to the position x and the time t which are the only independent variables. Natural boundary conditions Eq. (1-28a) and no mass flux from boundaries Eq. (1-28b), in one-dimensional study take the following form

$$\frac{\partial \bar{c}}{\partial x} = 0 \quad \text{at } t > 0, \quad x = 0 \text{ and } x = L \quad (3-1a)$$

$$\frac{\partial^3 \bar{c}}{\partial x^3} = 0 \quad \text{at } t > 0, \quad x = 0 \text{ and } x = L \quad (3-1b)$$

The initial condition used in our study is that we have a column that is filled by one fluid in one half and by another fluid in the other half. Since the fluids are immiscible, we

have an interface where fluids touch each other. In case only water and oil are present, we have a binary immiscible solution where only one scalar field of concentration, let us say water c_w can be defined. Then, the concentration of the other phase (oil) is clearly $c_o = 1 - c_w$. Hence, the initial condition pictures a sharp shock at interface where the concentration is discontinuous. Whereas the initial condition could not be used in this discontinuous form, we employ a hyperbolic form to smooth it;

$$c_{init} = \frac{c_{Max} + c_{Min}}{2} - \frac{c_{Max} - c_{Min}}{2} \tanh \left(\mathfrak{C} \left(x - \frac{L}{2} \right) \right) \quad (3-2)$$

where \mathfrak{C} has a constant value and signifies the degree of smoothness. c_{Max} and c_{Min} are the highest and lowest concentration values respectively at the both sides of the interface. In this study, the values for χ_{ij} are taken such that to evince a conceivable sharp interface between the immiscible fluids.

3-1-2 Numerical Solution Method

Many ideas for the numerical solution are taken from Chan & Rey (1995)[chan]. Although Galerkin's finite element is used in our study, nevertheless the method is slightly different from Cahn & Rey procedure. First of all it should be mentioned here, this numerical study is limited to binary solutions which we extend to multi-component afterwards. In order to have an easier test function to apply for Galerkin's method, we split up the CH equation into a system of equations as means to reduce the forth order term to the second order. Then CH equation is expressed as follows

$$\rho \frac{\partial c}{\partial t} = \nu \nabla \cdot \left\{ f_0''(c) \nabla c - \kappa \nabla w \right\} \quad (3-3a)$$

$$w = \Delta c \quad (3-3b)$$

After integration by part and implementation of the divergence theorem on Eq. (3-3a) and Eq. (3-3b), the following weak form is obtained to find $c(x, t)$, $c(x, 0) = c_{init}(x)$ and w , such that

$$\rho \int_{\Omega} \frac{\partial c}{\partial t} \varphi dA = -\nu \int_{\Omega} \left\{ f_0''(c) \nabla c - \kappa \nabla w \right\} \cdot \nabla \varphi dA \quad (3-4a)$$

$$\int_{\Omega} w \psi dA = - \int_{\Omega} \nabla c \cdot \nabla \psi dA \quad (3-4b)$$

for all test functions φ and ψ . The solution of the quantity is written as a linear combination of all values that the quantity has in every step size, and the function which corresponds to the position of that step size associated with its enclosing nodes. Therefore, the solution is expressed with the help of basis functions as

$$c(x, t) = \sum_{i=1}^n c_i(t) \varphi_i \quad (3-5a)$$

$$w(x, t) = \sum_{i=1}^n w_i(t) \psi_i \quad (3-5b)$$

where basis functions $\varphi = \varphi(x, y, z)$ & $\psi = \psi(x, y, z)$ depend on position and test functions are equal to the basis functions. In our one-dimensional study test functions only depend on one independent variable $\varphi = \varphi(x)$ and $\psi = \psi(x)$. Here, n is the number of step sizes which are created in computational domain by discretization. Linear test functions in the Galerkin's method for second order one-dimensional partial differential equations, are defined very easily on every node of computational domain, as indicated in Figure 3-1.

Substitution of Eq. (3-5a) and Eq. (3-5b) into Eq. (3-4a) and Eq. (3-4b) respectively,

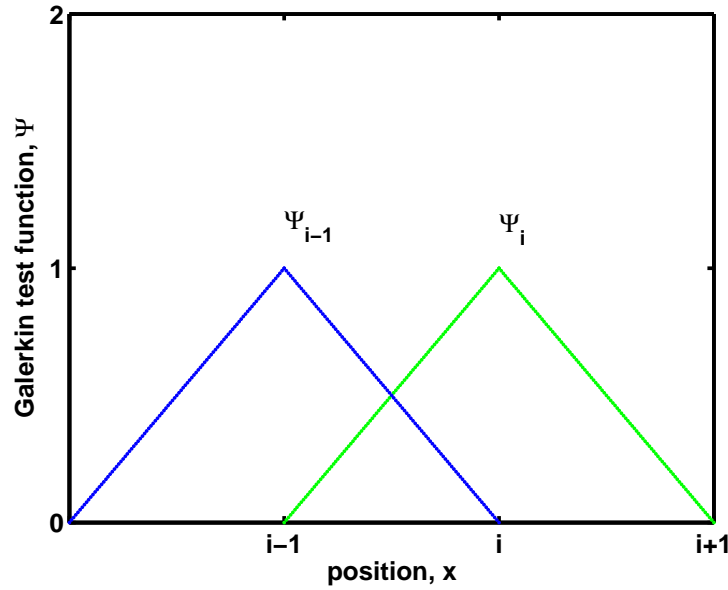


Figure 3-1: Galerkin linear test function, ψ vs. position x .

gives

$$\rho \sum_{i=1}^n c'_i(t) \int_{\Omega} \varphi_i \varphi_j dA = - \nu \sum_{i=1}^n c_i(t) \int_{\Omega} f''_0(\hat{c}_i) \nabla \varphi_i \nabla \varphi_j dA \quad (3-6a)$$

$$+ \nu \kappa \sum_{i=1}^n w_i(t) \int_{\Omega} \nabla \varphi_i \nabla \varphi_j dA$$

$$\sum_{i=1}^n c_i(t) \int_{\Omega} \nabla \psi_i \nabla \psi_j dA = - \sum_{i=1}^n w_i(t) \int_{\Omega} \nabla \psi_i \nabla \psi_j dA \quad (3-6b)$$

for all $j \in \{1, \dots, n\}$. \hat{c}_i is the concentration value at the specified step size which is normally equal to average of concentration values at its enclosed nodes.

In the leading equation, the terms including $\int_{\Omega} \varphi_i \varphi_j dA$ form the elements of Mass matrix \mathbf{M} . Similarly the Stiffness matrices $\mathbf{S}(c)$ and \mathbf{S} are constructed by the terms $\int_{\Omega} f''_0(\hat{c}_i) \nabla \varphi_i \nabla \varphi_j dA$ and $\int_{\Omega} \nabla \psi_i \nabla \psi_j dA$, respectively. Corresponding to Figure 3-1, the matrix elements will be zero if $|i - j| \geq 2$. Hence, matrices \mathbf{M} , $\mathbf{S}(c)$ and \mathbf{S} are tri-diagonal. Collecting all the equations together for the whole of domain, finally gives

$$\begin{pmatrix} \rho \mathbf{M} + \Delta t \nu \mathbf{S}(\underline{c}^m) & -\kappa \nu \Delta t \mathbf{S} \\ \mathbf{S} & \mathbf{M} \end{pmatrix} \begin{pmatrix} \underline{c}^{m+1} \\ \underline{w}^{m+1} \end{pmatrix} = \begin{pmatrix} \rho \mathbf{M} \underline{c}^m \\ \mathbf{0} \end{pmatrix} \quad (3-7)$$

where m is the time iterator that refers to the values at the present time. Note that \underline{w} and \underline{c} are the concentration profiles for one component associated with the node positions along the column. This differs from the \bar{c} which is used in Chapter 1 to denote the concentration vector of all components regardless of the computational domain. When the mixture contains more than two components, the same set of equations shall be written for the concentration profile of every constituent. More on this will be presented in the next section.

The $\mathbf{S}(\underline{c})$ elements contrary to \mathbf{S} and \mathbf{M} , are dependent on the concentration profile since the diffusivity factor $f_0''(\hat{c})$ is included. For the sake of simplicity and computation time, we compute the diffusivity factors in previous time step to avoid a non-linear problem. Later on, we discuss the advantages and disadvantages of the methods which are used to solve the non-linear CH problem compared to linear solution (see section 4-1).

3-2 Stefan Numerical Solution Technique

The same noted Galerkin's FEM is used here. Some minor changes are applied to cover the boundary conditions Eq. (1-34a) in accordance with the explicit definition of the interface position Eq. (1-34c) & Eq. (1-34c). Taking Figure 1-1 into consideration, solution requires to be defined in both zones individually by means of Galerkin basic functions,

$$c(x, t) = \sum_{i=1}^n c_i(t) \varphi_i + c_L \varphi_{n+1}(x) \quad \text{in } \Omega_1 \quad (3-8a)$$

$$c(x, t) = c_R \varphi_1(x) + \sum_{i=2}^{n+1} c_i(t) \varphi_i \quad \text{in } \Omega_2 \quad (3-8b)$$

c_L and c_R are binodal points. When we have $c_L < c_R$, the situations $c(x, t) \leq c_L$ in Ω_1 and $c(x, t) \geq c_R$ in Ω_2 hold, which renders the loss of regularity at domains. We consider each domain divided into n stepsizes, so we have $n + 1$ nodes. The weak form of Eq. (1-33a) is obtained just like that obtained for the CH equation on account of natural boundary condition Eq. (1-34a),

$$\int_{\Omega_i} \frac{\partial c}{\partial t} \varphi \, dx - \int_{\Omega_i} x_t \frac{\partial c}{\partial x} \varphi \, dx = - \int_{\Omega_i} f_0''(c) \frac{\partial c}{\partial x} \frac{\partial \varphi}{\partial x} \, dx \quad (3-9)$$

where $\Omega_i \in \{\Omega_1, \Omega_2\}$ and $x_t = \partial x / \partial t = x_t(x, t)$ is assumed to be a factor which represents relative movement of the isomorphic points in time due to the interface motion. Replacement of solutions Eq. (3-8a) and Eq. (3-8b) into weak form, gives the

conclusive expression for the dissipation in each domain

$$\sum_{i=1}^n c'_i(t) \int_{\Omega_1} \varphi_i \varphi_j dA - \sum_{i=1}^n c_i(t) \int_{\Omega_1} x_t \nabla \varphi_i \varphi_j dA - c_L \int_{\Omega_1} x_t \nabla \varphi_{n+1} \varphi_j dA \quad (3-10a)$$

$$= - \sum_{i=1}^n c_i(t) \int_{\Omega_1} f_0''(\hat{c}_i) \nabla \varphi_i \nabla \varphi_j dA - c_L \int_{\Omega_1} f_0''(\hat{c}_i) \nabla \varphi_i \nabla \varphi_j dA$$

$$\sum_{i=2}^{n+1} c'_i(t) \int_{\Omega_2} \varphi_i \varphi_j dA - \sum_{i=2}^{n+1} c_i(t) \int_{\Omega_2} x_t \nabla \varphi_i \varphi_j dA - c_R \int_{\Omega_2} x_t \nabla \varphi_{n+1} \varphi_j dA \quad (3-10b)$$

$$= - \sum_{i=2}^{n+1} c_i(t) \int_{\Omega_2} f_0''(\hat{c}_i) \nabla \varphi_i \nabla \varphi_j dA - c_R \int_{\Omega_2} f_0''(\hat{c}_i) \nabla \varphi_i \nabla \varphi_j dA$$

$$\forall j \in \{1, \dots, n\}$$

In case of immiscible fluids, the Eq. (3-10a) & Eq. (3-10b) fulfill the expectations of sharp interface between two zones providing so-called miscibility gap, $|c_L - c_R|$. The new place of interface can be traceable by use of Eq. (1-33b) as below

$$S^{k+1}(t) = S^k(t) - \Delta t \frac{[[f_0''(c) \frac{\partial c}{\partial x}]]}{[[c]]} \quad (3-11)$$

where $[[\]] = ()_{\Omega_1} - ()_{\Omega_2}$ denotes the jump of values across the interface. The velocity x_t has its maximum value at interface dS/dt and minimum value of zero at the no mass flux boundaries. In the numerical solution at initial step, the velocity term has no value. So we solve set of equations without velocity term and after calculation of the velocity profile, we repeat the whole process for initial step again.

Chapter 4

Results

4-1 The CH Binary Mixture

As it was stated in chapter 2 we focus our study mainly on the binary solutions in a one-dimensional domain. We consider two incompressible and immiscible fluids contacting together in a closed system at isothermal conditions. In fact, immiscible fluids diffuse into each other to a small extent. The effect of acceleration and conductivity is rather neglected and we assume that diffusion is the only cause of dissipation. The natural boundary conditions for each model are already discussed which are principally induced by a zero mass flux at the boundaries. The numerical calculation of the model is generalized for every immiscible system and the parameters are not chosen to represent some specific fluids. The initial condition describes two separated zones where each is filled by one of the fluids completely.

The first step is to smooth the discontinuities of the initial condition using Eq. (3-2). The type of smoothing could be applied by means of variety type of functions, like hyperbolic tangent, which is used in this study. Figure 4-1 displays the effect of different values of \mathfrak{C} on the steepness.

As an example of the numerical method which is discussed in section(3-1) for CH equation, the results for a hypothetical immiscible binary system look like Figure 4-2. As we see in results on Figure 4-2, the movement of the interface in early time steps is larger than at later stages. The same happens for diffusion through interface which decreases to a very insensible amount when the concentration gradients can not decay the total free energy and the solution essentially is stabilized (see Figure 4-3(b)). Figure 4-2 shows that the displacement of interface in the starting 5% of the total time ($t = 0.2$) is almost equal to half of the entire displacement (at $t = 3.5$).

In immiscible mixtures, the motion of interface could happen in case of non-symmetry. In CH equation κ brings the effect of the surface tensions into account. As we see in Figure 4-4 to have a continuous displacement of interface, the values of κ should not be less than a specific range of values. However, this range of values of the κ has to be

taken sufficiently small for the model to comprise an acceptable sharp interface. The CH equation Eq. (1-27b) fully supports mass conservation and it is already proved mathematically in section 2-1-1. To confirm it in our model numerically, the amount of mass is plotted as a function of time (see Figure 4-3(a)). Regardless of the small changes in total mass due to local errors, we see mass remains comprehensively constant in time which supports our theoretical considerations.

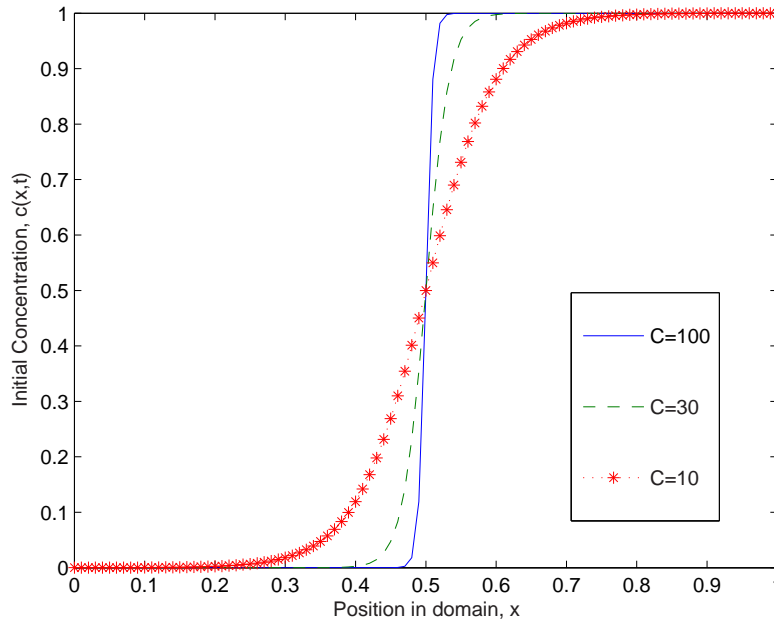


Figure 4-1: Different values of \mathcal{C} have a huge effect on the steepness. The higher the value of \mathcal{C} , the sharper is the interface. This study uses $\mathcal{C} = 100$.

Due to the stabilization, the total free energy of the system should reduce in time. The reduction is very fast at primary time steps, and rapidly starts to slow down at subsequent steps (see Figure 4-3(b)). The diffusion through the interface also has a same behavior of energy reduction. Energy decrease is proved theoretically for the CH equation in section 2-1-2 and confirmed here by the numerical results.

To avoid the non-linear system of equations resulting from $\mathbf{S}(\underline{c})$ in Eq. (3-7), $\mathbf{S}(\underline{c})$ is computed explicitly. To be exactly true, the diffusion factors $f_0''(\hat{c})$ should be computed implicitly which leads to a non-linear system of equations

$$\begin{pmatrix} \rho\mathbf{M} + \Delta t \nu \mathbf{S}(\underline{c}^{m+1}) & -\kappa \nu \Delta t \mathbf{S} \\ \mathbf{S} & \mathbf{M} \end{pmatrix} \begin{pmatrix} \underline{c}^{m+1} \\ \underline{\mathcal{E}}^{m+1} \end{pmatrix} = \begin{pmatrix} \rho\mathbf{M}\underline{c}^m \\ \mathbf{0} \end{pmatrix} \quad (4-1)$$

To solve the fully implicit version Eq. (4-1) we employed two different so-called predictor-corrector methods, Newton-Raphson and Picard. The idea in these methods is to first predict the answer explicitly and thereafter correct the answer to some extent which the error is negligible. The Full implicit solution of CH equation Eq. (4-1) stays stable in case the higher value of Δt is applied. Figure 4-5 compares the outcomes for

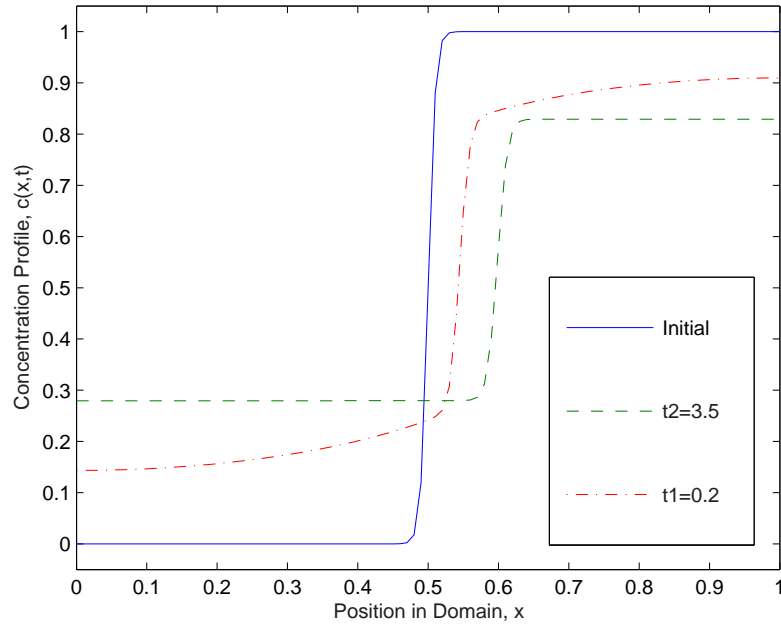
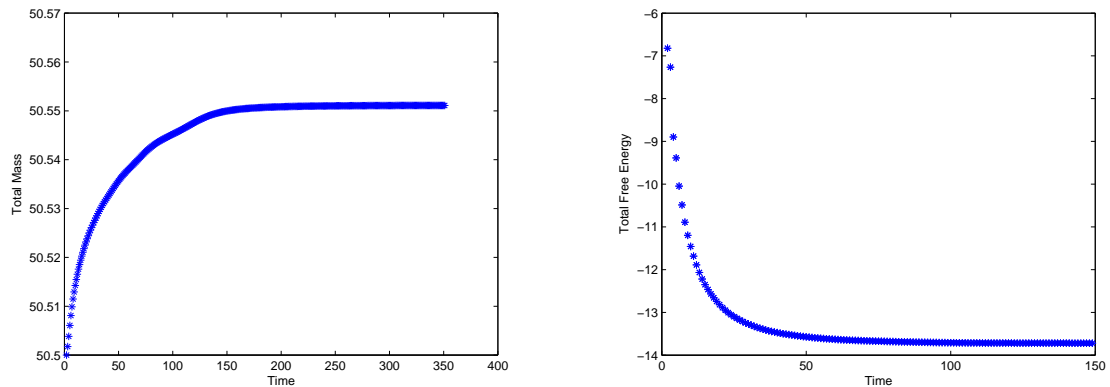


Figure 4-2: Numerical results of the CH equation at various times for two immiscible fluids with particular properties $\mathcal{N}_1 = 0.8$, $\mathcal{N}_2 = 1.3$, $\chi = 2.3 > \chi_{12}^{cr}$, $\kappa = 5 \times 10^{-6}$, $\nu = 1$. To get a stable numerical solution, computational domain ($L = 1$) is divided into 100 parts and $\Delta t = 0.01$.



(a) Mass is conserved in the numerical solution of the model as it is proved theoretically in section (2-1-1).

(b) Numerical demonstration of the free energy decay in the model.

Figure 4-3: Numerical verification of energy decline and mass conservation for the CH equation.

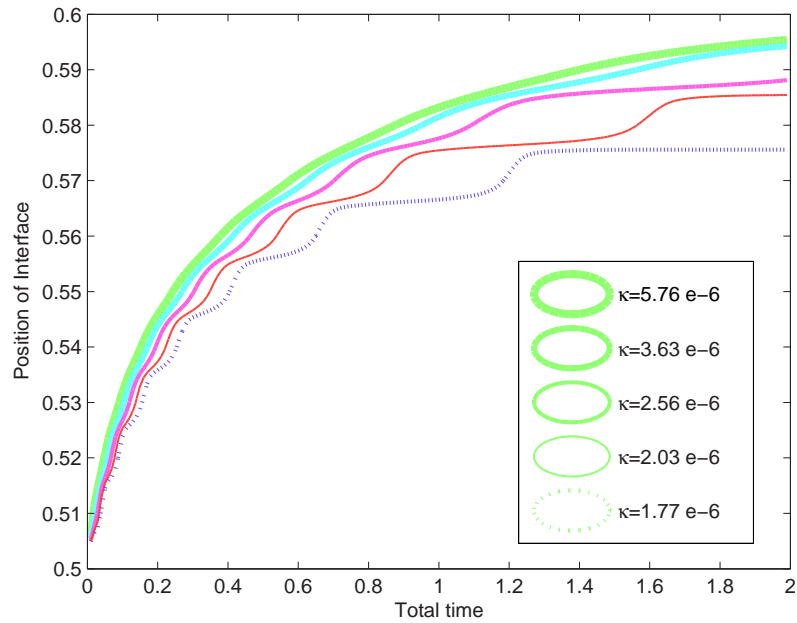


Figure 4-4: Interface movement results from CH equation with respect to different values of κ .

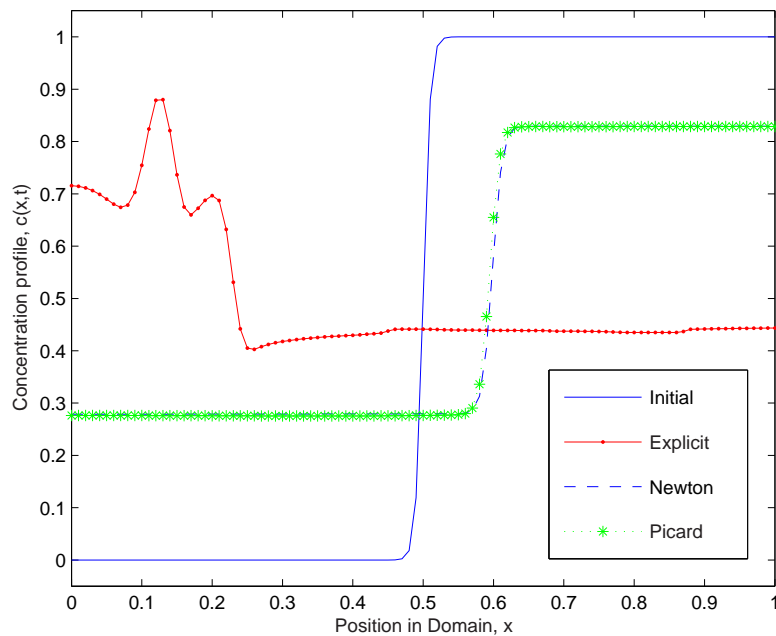


Figure 4-5: Comparison between the result of the non-linear solution methods and the linear one when $\Delta t = 0.03$ is large.

each method when Δt is increased three times more $\Delta t = 0.03$. The results show that the two Newton-Raphson and Picard methods for the non-linear solution of Eq. (4-1) give rather same answer but the solution by an explicit method of Eq. (3-7) gives an unstable result. Our suggestion is to use an explicit solution with sufficiently small Δt to prevent numerical instability, because the implicit non-linear methods are very time-consuming and computationally expensive, specially for three spatial dimensions. Anyhow, in case to use one of them we suggest to employ Newton-Raphson which is slightly faster and has trustworthy results.

4-2 Multi-component Case

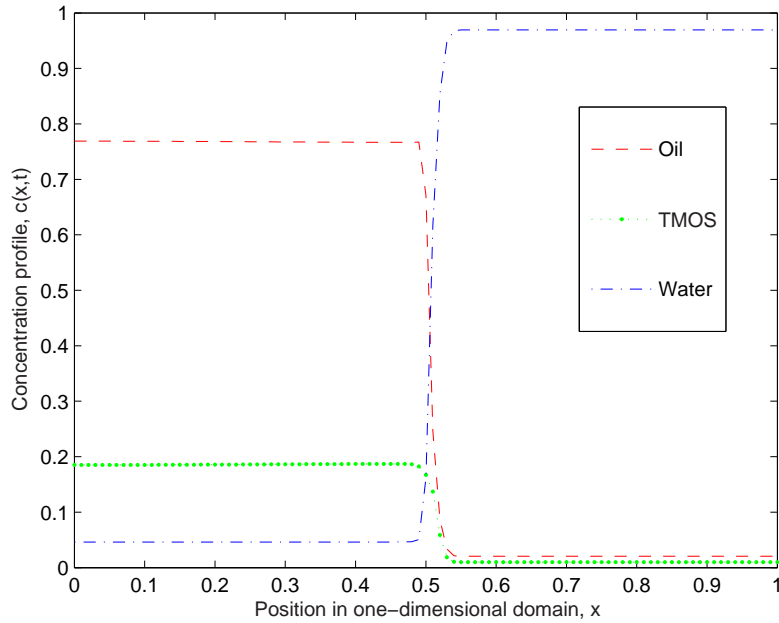


Figure 4-6: Ternary mixture behavior based on Eyre expression Eq. (2-9) which is extension of the Cahn-Hilliard formula for multi-component mixtures.

The numerical procedure to solve the system of equations for multi-component mixture is approximately the same as that for the binary case, however it demands more computation time. In our hypothetical case of a TMOS/oil/water system, mainly water and oil constitute the phases and the third component, TMOS here as a organic chemical, is only soluble in the oil. If the first term on the right-hand side of Eq. (3-7) is considered as a $[2n \times 2n]$ matrix for binary case, for the mixture with $N + 1$ components it is a $[2N(n) \times 2N(n)]$ matrix. The elements are defined from Eq. (2-12) by the help of Eq. (2-13). Figure 4-6 demonstrates the solution of Eyre's expression for a ternary mixture where the third component (TMOS) is considered to be soluble only in oil. So the interaction parameter of TMOS/oil is fairly small compared to water/oil and TMOS/water ($\chi_{To} = 0.8$, $\chi_{wo} = 2.7$, $\chi_{Tw} = 2.5$). The non-localities Γ_{ij} are assumed

casually as very small numbers between 10^{-4} and 5×10^{-4} for the sake of keeping the interface sharp. Also the size of the molecules of oil and TMOS are assumed to be larger than water ($\mathcal{N}_o = 1.65$, $\mathcal{N}_T = 1.95$, $\mathcal{N}_w = 1$). Initially in the mixture, at one side of the interface there is %20 of soluble TMOS in %80 oil without any water and the other side contains only water.

We know organic chemical TMOS is soluble in oil and reacts after diffusion into water to form methanol and silicic acid. So, for a complete model a reaction term requires to be introduced into our system of equations to deplete the diffused TMOS inside the water phase. This reaction term, which plays a role in the water-phase, is not incorporated in the present study.

4-3 Stefan Problem for the Binary Solution

To avoid the negative values of the diffusion factors in unstable region and strange behavior of phases in metastable region which are mainly located between binodal points, we decide to look at the loss of regularity apart from unstable and metastable zones. For this reason, we take these zones as parts of the interface itself. Therefore, we neglect the weak non-locality term with κ because it only points to dispersion at the interface in CH equation and has a minor effect on localized dissipation. According to individual investigation of the behavior of the domains in this method, we need to track the position of interface by use of combination of the values jump across it and its velocity, Eq. (3-11). The application of Stefan problem on the same computational domain which is used for CH equation with use of similar boundary and initial conditions gives the results as it is shown in Figure 4-7. Same to the Figure 4-2 in the starting 5% of the total time, the interface shifts as equal as it shifts in rest of the total time. Mass conservation and energy decay of Stefan problem already discussed theoretically in section 2-3-1. Herewith we verify them in our numerical model. As Figure 4-8(a) shows the mass is conserved in Stefan model as accurately as it is in CH equation Figure 4-3(a). We have two explicit terms in Stefan equations Eq. (3-10a) & Eq. (3-10b), velocity x_t and diffusivity factor $f_0''(\bar{c})$. To be more accurate we need to solve these equations nonlinearly by means of Newton-Raphson or Picard methods which is not done in this study.

Energy reduction which is shown here in Figure 4-8(b) for Stefan problem, indicates that Eq. (2-25) is satisfied by our model. To investigate it for our case (Figure 4-7), we substitute the values of binodal points, $c_L = 0.2479$ and $c_R = 0.8443$, into Eq. (2-25). The interface moves to to the right, then the value of $S^\infty - S^0$ is always positive. From numerical solution $S^{350} - S^0 = 0.0921$ and $f(c_L) - f(c_R) = -0.0692$ which implies a sufficient condition Eq. (2-25) for the energy decrement.

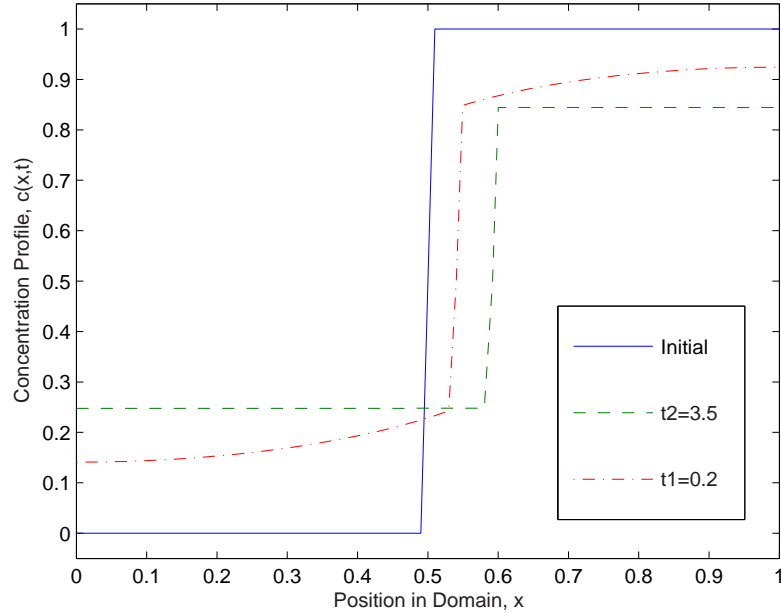
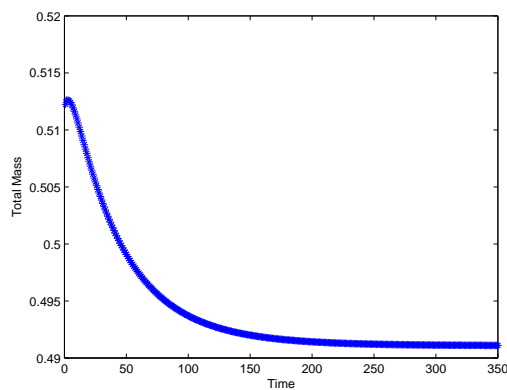
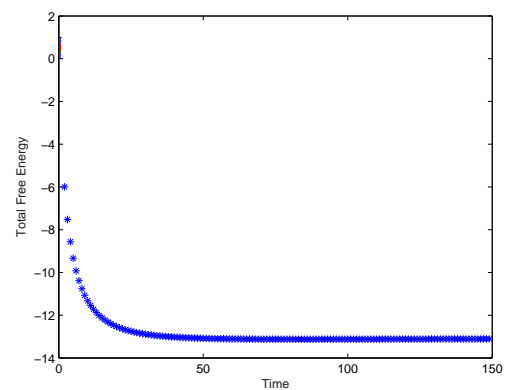


Figure 4-7: Numerical result of the Stefan problem for two immiscible fluids with particular properties $\mathcal{N}_1 = 0.8$, $\mathcal{N}_2 = 1.3$, $\chi = 2.3 > \chi_{12}^{cr}$, $\kappa = 0$. Computational domain ($L = 1$) is divided to 100 parts and $\Delta t = 0.01$. The stability of numerical solution is not dependent to the values of Δt and Δx .



(a) Mass is conserved in numerical solution of the Stefan problem.



(b) Numerical demonstration of the free energy decay in the Stefan model.

Figure 4-8: Numerical illustration of energy decline and mass conservation for a Stefan problem.

4-4 Comparison between a Stefan Problem and the CH Model

As already mentioned, we used Galerkin's FEM in this study for both models. Fortunately the results from models are quite comparative. Nevertheless, depending on the situation, limitations, priorities and posteriorities one of those models might be preferred more. The remarks about CH model are as following:

- Choosing a proper test function for fourth order CH equation and followed numerical procedure takes more effort than for second order Stefan problem, nevertheless when it is done we do not need to track the interface and rearrange all the grids in computational domain in every time cycle. So CH model is easier to be figured out numerically.
- Comparison between Figure 4-3(a) and Figure 4-8(a) shows that both CH model and Stefan problem are very accurate in order to consider mass conservation. In the CH model, local errors slightly change the total mass in an increasing order but in the Stefan problem, the total mass is decreased by the errors for a little.
- Considering Eq. (3-6a) & Eq. (3-6b) for the CH model and Eq. (3-10a), Eq. (3-10a) & Eq. (3-11) for the Stefan problem, the numerical procedure seems much simpler for CH model than Stefan problem. For this reason, it is easier to solve nonlinear CH equation than Stefan problem. However the computation times are almost equal for our similar hypothetical case.
- The stability of the numerical solution is extremely sensitive to the values of Δt in relation to Δx . As it was mentioned we can choose higher values for this parameters but we need to solve the non-linear equation which is relatively time and computationally expensive.
- We need to compromise on the value of weak non-locality κ for our case. The value first is suggested to neutralize the effect of concavity in free energy diagram. Later on the value of κ considered to be relative to surface tension at the interface [1],[4]. But for our hypothetical case, we need to find the value of κ in order to preserve the sharp interface between immiscible fluids.
- The CH model requires the discontinuities of the initial condition to be smoothed which is an intuitive way to have a reasonable results. The smoothing process prevents from a sharp interface to be considered initially.

The points about Stefan problem which is resulting from numerical process and formulation are as follows:

- We do not need to compromise on the value of weak non-locality κ . As $\kappa \rightarrow 0$ and the behavior of domains are investigated separately from unstable region, its value is considered to be zero.
- The stability of solution is independent to the values of Δt and Δx .

- Contrary to CH model in which the position is captured automatically, the followed numerical procedure to investigate the behavior of the deformed domains resulting from the interface shift is quit challengeable.
- The essential boundary conditions which implies the fixed values of concentration (binodal values) across the interface during the simulation time, prevents from a smooth dissipation around the interface compared to other points of domain. Thus, the consequences of having essential boundary conditions at the sides of the interface in order to have the loss of regularity in the domains, are not very conventional.
- The very sharp interface which is manually treated and which separates computational domains, prevents the concentration profile to have the range of values which are inside the metastable or unstable regions. In another words, the region between binodal points is completely skipped by assuming it as a part of the interface.

The results of both models are compared in Figure 4-9 and we see that both methods yield approximately same results. So the use of each method is totally depends on the priorities.

Figure 4-10 shows that the movement of interface in both methods is quite similar.

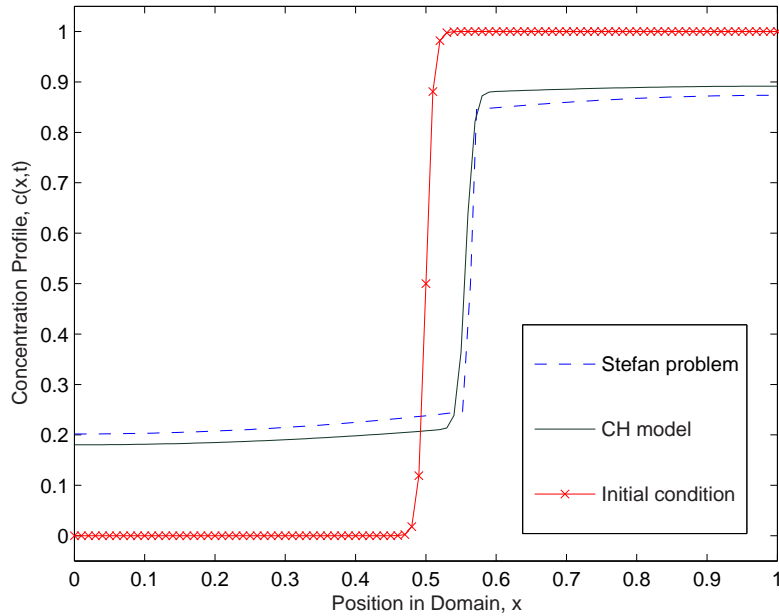


Figure 4-9: Numerical results of the Stefan problem and the CH equation for two immiscible fluids after a certain time ($t = 1$) with particular properties $\mathcal{N}_1 = 0.8$, $\mathcal{N}_2 = 1.3$, $\chi = 2.3 > \chi_{12}^{cr}$. Computational domain ($L = 1$) is divided to 100 parts and $\Delta t = 0.01$. $\kappa = 5 \times 10^{-6}$ is considered for CH equation.

Comparison between the results of two models, illustrates that both methods could be

used in order to simulate the behavior of immiscible fluids in the mixture. Still many improvements can be applied in the numerical solution of both models to reach to a closer match.

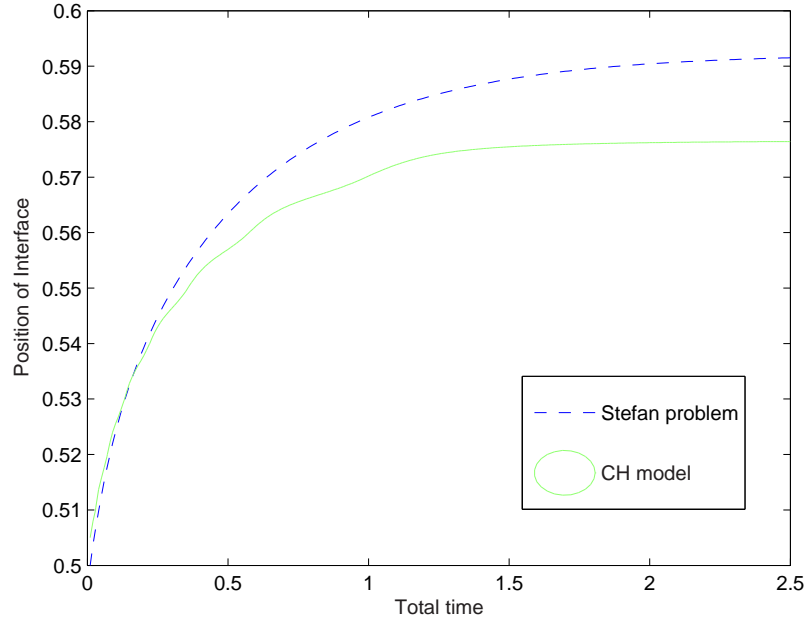


Figure 4-10: Displacement of the interface as a result of applying the Stefan problem and the CH equation on two immiscible fluids after a certain time ($t = 1$) with particular properties $\mathcal{N}_1 = 0.8$, $\mathcal{N}_2 = 1.3$, $\chi = 2.3 > \chi_{12}^c$. Computational domain ($L = 1$) is divided to 100 parts and $\Delta t = 0.01$. $\kappa = 5 \times 10^{-6}$ is considered for CH equation.

Chapter 5

Conclusions

The used Finite Element method for the Cahn-Hilliard equation produces reliable results and provides the capabilities of expansion as means to develop for higher dimensions. The extension to multi-component Cahn-Hilliard equations is straightforward. By a rigorous mathematical analysis, it has been shown that the solutions to the Cahn-Hilliard equations are mass-conserving and satisfy the requirement of energy decrease. This has been done for the case of natural boundary conditions.

Furthermore, the solutions of the Cahn-Hilliard equation are demonstrated to coincide well with the solutions of a Stefan problem, for which we also prove mass conservation and energy decrease.

Each model has its own cons and pros. The Cahn-Hilliard model is simpler to be expanded into the higher dimensions, gives smoother solution and tracks automatically the interface position. But in another hand, it is conditionally stable and the values of uncomprehended parameters like κ play an important role in which to achieve a reasonable results. The Stefan problem does not have the stability issues as well as compromising problems on the values of some parameters. However, the description of the essential conditions on the interface is rather unconventional and dealing with the continuous deformation of the computational domain due to the displacement of the interface is very challengeable in programming point of view. Since both models approximately lead to the same results, it is needed to consider the priorities, the limitations and the requirements for each case study in order to choose the more appropriate model.

Bibliography

- [1] K. Binder. *Collective diffusion, nucleation, and spinodal decomposition in polymer mixtures*. J. Chem. Phys. 79, 1983.
- [2] G. Brown and J. Chem A. Chakrabarti. Phys. 98 2451, 1993.
- [3] A. Chakrabarti. Phys. Rev. B 45 9620, 1992.
- [4] P.G. de Gennes. *Dynamic of fluctuations and spinodal decomposition in polymer blends*. J. Chem. Phys. 72, 1980.
- [5] David Qiwei He E.Bruce Nauman. *Nonlinear diffusion and phase separation*. Chemical Eng. Science 56 1999-2018, 2001.
- [6] Teixeira da Silveira Filho E.V.I. de Mello. *Numerical study of the Cahn-Hilliard equation in one, two and three dimensions*. Physica A, 347, pp. 429-443, 2005.
- [7] David J. Eyre. *System of Cahn-Hilliard Equations*. Applied Math. Vol. 53, No 6 1686-1712, 1993.
- [8] C. Vuik F.J. Vermolen. *Solution of vector Stefan problem with cross-diffusion*. Journal of Comp. and Applied Math. 176 179-201, 2005.
- [9] S. van der Zwaag F.J. Vermolen, C. Vuik. *Cross-diffusion controlled*. Material Science and Eng. A347 265-279, 2003.
- [10] Flory P. J. *Principles of polymer chemistry*. Cornell University Press, NY, 1953.
- [11] A. Chakrabarti J.D. Gunton, R. Toral and M. Muthukumar. Phys. Rev. Lett. 63 2072, 1989.
- [12] A. Chakrabarti J.D. Gunton, R. Toral and M. Muthukumar. J. Chem Phys. 92 6899, 1990.

-
- [13] M. San Miguel J.D. Gunton and P.S. Sahni. *Phase Transitions and Critical Phenomena*. Academic press, London, vol. 8, 1983.
 - [14] Cahn JW and Hilliard JE. *Free energy of a non-uniform system. I. Interfacial free energy*. J. Chem Phys 28, 258-267, 1958.
 - [15] J. Lowengrub and L. Truskinovsky. *Quasi-incompressible Cahn-Hilliard fluids and topological transitions*. The Royal Society. 454, 2617-2654, 1998.
 - [16] R.L. Pego. *Front migration in the nonlinear Cahn-Hilliard equation*. Proceedings of the Royal Society of London Ser. A, 422, pp. 261-278, 1989.
 - [17] Alejandro D. Rey Philip K. Chan. *A numerical method for nonlinear Cahn-Hilliard equation with nonperiodic boundary conditions*. Computational Material Science 3, 377-392, 1995.